NAS1.26:3412

ORIGINAL

NASA Contractor Report 3412

COMPLETED

Calculation of Two-Dimensional Inlet Flow Fields by an Implicit Method Including Viscous Effects - User's Manual

Sedat Biringen and Oden J. McMillan

CONTRACT NAS1-15951
MAY 1981

NASA

NASA Contractor Report 3412

Calculation of Two-Dimensional Inlet Flow Fields by an Impact Method Including Viscous Effects - User's Manual

Sedat Biringen and Oden L. McMillan
Nielsen Engineering & Research, Inc.
Mountain View, California

Prepared for
Langley Research Center
under Contract NAS1-15951

National Aeronautics
and Space Administration

**Scientific and Technical
Information Branch**

1981

I

BIANK PAGE

SUMMARY

Inlet flow fields for airbreathing missiles are calculated by the adaptation of a two-dimensional computational method developed for the flow around airfoils. A supersonic free stream is assumed to allow the forebody calculation to be uncoupled from the inlet calculation. The inlet calculation employs an implicit, time-marching finite-difference procedure to solve the thin-layer Navier-Stokes equations formulated in body-fitted coordinates. The mathematical formulation of the problem and the solution algorithm are given. Numerical stability and accuracy as well as the initial and boundary conditions are discussed. Instructions for program use and operation along with the overall program logic are also given.

1. INTRODUCTION

This report consists of the technical explanation of the computer code that is employed to calculate two-dimensional (planar) inlet flow fields in a supersonic free stream including viscous effects. This code is a modified version of the program that was developed and used in reference 1 to calculate external flows over two-dimensional airfoils. In earlier reports (refs. 2 and 3), a detailed discussion of the inviscid version of this code (the Euler code) and the details of the grid-generation routine are given. In reference 4, preliminary applications of the method to inviscid flow in two-dimensional inlets are described.

In the following sections of this report, the version of the code including viscous effects is explained in detail: the mathematical formulation of the program is given and the computational algorithm as well as program logic are explained. A listing of the program and the output for a test case are contained in reference 5. Applications of this code and the Euler code to an inlet representative of current design practice and an assessment of the utility of the codes for such use (including convergence and stability behavior) are described in reference 6.

2. FORMULATION OF THE PROBLEM

In this section the governing equations (Navier-Stokes equations with the thin-layer approximation) for flow fields in two-dimensional inlets are given. Turbulent closure approximations are described, and boundary and initial conditions as well as the numerical solution procedure and its stability are discussed.

2.1 Governing Equations

The Navier-Stokes equations in Cartesian coordinates for plane two-dimensional flows can be written in conservation-law form in terms of non-dimensional variables for a perfect gas without external forces as (refs. 1,7)

$$\partial_t \vec{q} + \partial_x \vec{E} + \partial_y \vec{F} = Re^{-1}(\partial_x \vec{R} + \partial_y \vec{S}) \tag{1}$$

where

$$\vec{q} = \begin{pmatrix} \rho \\ \rho u \\ \rho v \\ e \end{pmatrix}, \quad \vec{E} = \begin{pmatrix} \rho u \\ \rho u^2 + p \\ \rho uv \\ u(e + p) \end{pmatrix}, \quad \vec{F} = \begin{pmatrix} \rho v \\ \rho uv \\ \rho v^2 + p \\ v(e + p) \end{pmatrix},$$

$$\vec{R} = \begin{pmatrix} 0 \\ \tau_{xx} \\ \tau_{xy} \\ R_4 \end{pmatrix}, \quad \vec{S} = \begin{pmatrix} 0 \\ \tau_{xy} \\ \tau_{yy} \\ S_4 \end{pmatrix}$$

with

$$\tau_{xx} = (\lambda + 2\mu)u_x + \lambda v_y, \quad \tau_{xy} = \mu(u_y + v_x),$$

$$\tau_{yy} = (\lambda + 2\mu)v_y + \lambda u_x,$$

$$R_4 = u\tau_{xx} + v\tau_{xy} + \kappa P_r^{-1}(\gamma - 1)^{-1}\partial_x a^2$$

$$S_4 = u\tau_{xy} + v\tau_{yy} + \kappa P_r^{-1}(\gamma - 1)^{-1}\partial_y a^2$$

and

$$p = (\gamma - 1)[e - 0.5\rho(u^2 + v^2)] \tag{2}$$

In these equations u and v are the velocities along the x and y coordinates respectively, p is the pressure, ρ is the density and e is the total energy per unit volume. The sound speed, a is given by $a^2 = \gamma(\gamma-1)\left(\frac{e}{\rho} - 0.5(u^2+v^2)\right)$ and Pr is the Prandtl number. Note that according to Stokes' hypothesis $\lambda = (-2/3)\mu$. The reference quantities are arbitrarily selected but the Reynolds number (Re) is defined in terms of these quantities. In order to use a body-fitted coordinate system, the governing equations are rewritten subject to the general transformation.

$$\begin{aligned} \xi &= \xi(x,y,t) \\ \eta &= \eta(x,y,t) \\ \tau &= t \end{aligned} \tag{3}$$

where ξ is the coordinate along the body and η is the coordinate perpendicular to the body. In addition to this transformation, if the governing equations are simplified with the "thin-layer" approximation (ref. 8), the following equation is obtained

$$\partial_\tau \hat{q} + \partial_\xi \hat{E} + \partial_\eta \hat{F} = R_e^{-1}\partial_\eta \hat{S} \tag{4}$$

where

$$\hat{q} = \vec{q}/J \quad , \quad \hat{E} = (\xi_t q + \xi_x E + \xi_y F)/J$$
$$\hat{F} = (\eta_t \vec{q} + \eta_x \vec{E} + \eta_y \vec{F})/J$$

$$Re^{-1}\partial_\eta \hat{S} \equiv Re^{-1}\partial_\eta J^{-1}\begin{Bmatrix} 0 \\ \mu(\eta_x^2+\eta_y^2)u_\eta + (\mu/3)\eta_x(\eta_x u_\eta+\eta_y v_\eta) \\ \mu(\eta_x^2+\eta_y^2)v_\eta + (\mu/3)\eta_y(\eta_x u_\eta+\eta_y v_\eta) \\ \kappa P_r^{-1}(\gamma-1)^{-1}(\eta_x^2+\eta_y^2)\,{}_\eta a^2 \\ \quad + \mu(\eta_x^2+\eta_y^2)(u^2+v^2)_\eta/2 \\ \quad + (\mu/3)(\eta_x u+\eta_y v)(\eta_x u_\eta+\eta_y v_\eta) \end{Bmatrix}$$

Here J is the transformation Jacobian given as

$$J = \xi_x\eta_y - \xi_y\eta_x = 1/(x_\xi y_\eta - x_\eta y_\xi) \tag{5}$$

whereas ξ_t, ξ_x etc., are the metrics formed from the derivatives of x_τ, x_ξ, etc., using the relations

$$\begin{aligned} \xi_x &= Jy_\eta & \eta_x &= -Jy_\xi \\ \xi_y &= -Jx_\eta & \eta_y &= Jx_\xi \\ \xi_t &= -x_\tau\xi_x - y_\tau\xi_y & \eta_t &= -x_\tau\eta_x - y_\tau\eta_y \end{aligned} \tag{6}$$

We now define velocities along the ξ and η coordinates

$$\begin{aligned} U &= \xi_t + \xi_x u + \xi_y v \\ V &= \eta_t + \eta_x u + \eta_y v \end{aligned} \tag{7}$$

Using these velocities, $\hat{E}$ and $\hat{F}$ can be written as

$$\hat{E} = J^{-1}\begin{pmatrix} \rho U \\ \rho uU+\xi_x p \\ \rho vU+\xi_y p \\ (e+p)U-\xi_t p \end{pmatrix}, \quad \hat{F} = J^{-1}\begin{pmatrix} \rho V \\ \rho uV+\eta_x p \\ \rho vV+\eta_y p \\ (e+P)V-\eta_t p \end{pmatrix} \tag{8}$$

The inlet flow-field solution is obtained as the steady-state solution of the time-marching method employed to solve equation (4).

It should be noted that the thin-layer approximation neglects diffusion along the coordinate parallel to the body surface; all three momentum equations are retained and no assumption is made about the pressure. This feature enables the use of a single set of equations in attached and separated flow situations.

2.2 The Turbulence Model

Practical operational regimes for air-breathing missiles necessitate the use of a closure model to account for effects of transition and turbulence. In this code the thin-layer eddy-viscosity model of reference 8 is used. This model is a modified version of the two-layer eddy-viscosity model which was first proposed in reference 9. The modifications, which remove the necessity of locating the boundary-layer edge, consist of using the vorticity distribution to determine the characteristic length scale of the flow field. The Prandtl-van Driest formulation is used to damp the eddy-viscosity in the laminar sublayer.

The basic principle of the two-layer eddy-viscosity model is to simulate the effects of turbulence in terms of an eddy-

viscosity coefficient, μ_t. Hence the molecular viscosity coefficient, μ, that appears in the Navier-Stokes equations is replaced by $\mu + \mu_t$, and μ_t is calculated separately for the inner and outer regions of the boundary layer, i.e.

$$\mu_t = \begin{cases} (\mu_t)_{inner} & y \leq y_{crossover} \\ (\mu_t)_{outer} & y > y_{crossover} \end{cases} \tag{9}$$

where y is the normal distance from the wall and $y_{crossover}$ is the smallest value of y at which values from the inner and outer formulas are equal.

The Prandtl-Van Dreist formulation is used in the inner region to damp μ_t,

$$(\mu_t)_{inner} = \rho \ell^2 |\omega| \tag{10}$$

where ℓ (the turbulence length scale) is defined as

$$\ell = ky[1 - \exp(-y^+/A^+)] \tag{11}$$

Here $|\omega|$ is the magnitude of the vorticity vector and for two-dimensional flows is given as

$$|\omega| = \sqrt{\left(\frac{\partial u}{\partial y} - \frac{\partial v}{\partial x}\right)^2} \tag{12}$$

and

$$y^+ = \frac{\rho_w u_\tau y}{\mu_w} = \frac{\sqrt{\rho_w \tau_w} y}{\mu_w} \tag{13}$$

The outer layer eddy-viscosity coefficient is calculated from

$$(\mu_t)_{outer} = KC_{CP} F_{WAKE} F_{KLEB}(y) \tag{14}$$

where K is the Clauser constant, C_{CP} is an additional constant, and

$$F_{WAKE} = \left\{ \begin{matrix} \text{or} \\ C_{WK} \end{matrix} \begin{matrix} y_{MAX} F_{MAX} \\ y_{MAX} u_{DIF}^2 / F_{MAX} \end{matrix} \right\} \text{ the smaller} \tag{15}$$

The quantities y_{MAX} and F_{MAX} are determined from the function

$$F(y) = y|\omega|[1 - \exp(-y^+/A^+)] \tag{16}$$

The quantity F_{MAX} is the maximum value of F(y) that occurs in a profile and y_{MAX} is the value of y at which it occurs. The function $F_{KLEB}(y)$ is the Klebanoff intermittency factor given by

$$F_{KLEB}(y) = \left[1 + 5.5 \left(\frac{C_{KLEB} y}{y_{MAX}} \right)^5 \right]^{-1} \tag{17}$$

The quantity u_{DIF} is the difference between maximum and minimum total velocity in the profile (i.e., at a fixed x station)

$$u_{DIF} = \left(\sqrt{u^2 + v^2}_{MAX} - \sqrt{u^2 + v^2}_{MIN} \right) \tag{18}$$

The second term in u_{DIF} is taken to be zero (except in wakes).

The outer formulation (eqs. (14) and (15)) can be used in both attached and separated boundary layers.

In this model the effect of transition to turbulence is simulated by setting μ_t equal to zero everywhere in a profile for which the maximum tentatively computed value of μ_t from the foregoing relations is less than a specified value, that is,

$$\mu_t = 0 \quad \text{if} \quad (\mu_t)_{\substack{\text{max in} \\ \text{profile}}} < C_{MUTM}\mu_\infty \tag{19}$$

The constants appearing in the foregoing relations have been determined by requiring agreement with the formulation of reference 8 for constant pressure boundary layers at transonic speeds. The values thus determined are

$$A^+ = 26$$

$$C_{CP} = 1.6$$

$$C_{KLEB} = 0.3$$

$$C_{WK} = 0.25$$

$$k = 0.4$$

$$K = 0.0163$$

$$P_r = 0.72$$

$$P_{rt} = 0.9$$

$$C_{MUTM} = 14$$

2.3 Boundary and Initial Conditions

In the problem under consideration there are four types of boundary conditions (fig. 1). These are solid boundaries, inflow boundaries, outer boundaries and outflow boundaries.

Along the cowl surface and the ramp surface the no-slip viscous boundary condition is satisified, i.e. U = 0 and V = 0. The pressure on the body surface is found from the normal momentum equation. This gives

$$P_\xi(\eta_x\xi_x+\eta_y\xi_y) + P_\eta(\eta_x^2+\eta_y^2) = 0 \qquad (20)$$

Throughout the integration procedure values of ρ at the advanced time step (ρ^{n+1}) are assumed equal to values of ρ at the current time step (ρ^n) on the flow-field boundaries; the latter are obtained by linear extrapolation from the interior. This simplifies the procedure for implementing the boundary conditions but results in first-order accuracy in time on the boundaries.

Free stream values are specified at the inflow and outer boundaries. These may be non-uniform values as obtained from a solution for a forebody as described in reference 5. In the case of a solution including the effects of a forebody, the outer boundary is extended such that it contains the shock from the forebody. For computational economy in the use of mesh points in the work done to date, the inflow boundary has been located a short distance downstream of the leading edge of the ramp. This requires special treatment for the mesh points on the inflow boundary which are downstream of the ramp-leading-edge shock. This treatment is discussed below under the paragraph dealing with initial conditions.

The outflow boundary conditions on the portion of the outflow boundary external to the inlet are calculated by zeroth-

order extrapolation from the interior. On that portion inside the inlet duct, the boundary conditions are specified according to whether the condition being calculated is supercritical or subcritical. In the case of supercritical operation, the flow field variables are again calculated by zeroth-order extrapolation from the interior. For subcritical operation (subsonic outflow) a set of boundary conditions are incorporated which are obtained from the steady-state forms of the governing equations assuming uniform parallel outflow. To allow the use of this assumption, a constant-area section is added to the downstream portion of the inlet duct such that $v = 0$. Back pressure is prescribed consistent with subsonic outflow (constant along y-direction), and u and ρ are found by zeroth-order extrapolation from the interior. The energy, e, is calculated from the values of u, ρ and p. We have found empirically that in order to conserve total enthalpy for a subcritical calculation, the high pressure boundary condition has to be introduced over some 300 time steps. A branching is also provided to test whether the flow is subsonic or supersonic at the outflow boundary (the gradual increase in pressure, of course, will make the flow subsonic gradually). If at a particular time step the flow is supersonic, all the variables are found by zeroth-order extrapolation, otherwise the above subsonic conditions are imposed.

The initial conditions are specified by using either the impulsive initial condition, i.e., free-stream conditions are imposed throughout the flow field,or the final solution of a previously calculated flow field is used. When starting from free-stream conditions, inviscid values calculated from 2-D shock theory are used at the 3-5 points on the inflow boundary that are downstream of the ramp shock. No allowance is made for the ramp boundary layer at the inflow boundary.

2.4 Solution Procedure and the Numerical Schemes

In the solution procedure employed to integrate equation (4) a temporal linearization process is employed. In order to employ this on the vector terms of equation (4) one needs to evaluate the Jacobian Matrices $\hat{A} \equiv \partial\hat{E}/\partial\hat{q}$ and $\hat{B} \equiv \partial\hat{F}/\partial\hat{q}$. The flux vectors $\hat{E}$ and $\hat{F}$ are both linear combinations of $\vec{q}$, $\vec{E}$, and $\vec{F}$ (ref. 1). The viscous term is linearized by using the principle of homogeneity (ref. 1) such that

$$\hat{S}^{n+1} = \hat{S}^{n} + J^{-1}\,\hat{M}^{n}\,\hat{q}^{n+1} \tag{21}$$

where $\hat{M}$ is a 4x4 matrix whose elements are functions of $\vec{q}$.

In the solution procedure, after approximate factorization the linearized equations are cast into delta-form (ΔF) algorithm (refs. 1, 10). This algorithm is non-iterative, and requires the inversion of two-block-tridiagonal (4x4) coefficient matrices at each time step in the integration procedure at only the interior points. References 1, 4, 10, 11 and 12 contain detailed descriptions and various applications of the delta-form AF algorithm, hence here we outline it only briefly. The delta-form AF algorithm can be used either with trapezoidal or Euler temporal implicit differencing and reads

$$\begin{aligned}(I+h\delta_{\xi}\hat{A}^{n})(I+h\delta_{\eta}\hat{B}^{n}+h\delta_{\eta}\hat{M}^{n})(\hat{q}^{n+1}-\hat{q}^{n}) \\ = -\Delta t(\delta_{\xi}\hat{E}^{n}+\delta_{\eta}\hat{F}^{n}-R_{e}^{-1}\delta_{\eta}\hat{S}^{n}) - \alpha\Delta t(\delta_{\xi\xi\xi\xi}+\delta_{\eta\eta\eta\eta})\hat{q}^{n}\end{aligned} \tag{22}$$

Here δ_{ξ} and δ_{η} are second-order central-difference operators, Δt is the integration step size, and $h = \Delta t$ or $\Delta t/2$ for first-order or second order two-level time differencing, respectively. The fourth-order smoothing terms are added to the RHS of the difference equation both to overcome non-linear instability

and to damp short wave lengths (refs. 1, 10 and 11). It is generally desirable to add the smoothing term in terms of both explicit and implicit portions. The explicit part suppresses non-linear instabilities whereas the implicit part enables the use of $\alpha \sim 0(\Delta t)$ for very large Δt where α is the artificial viscosity coefficient. In the current work, these terms have been included in a pseudo-implicit manner by inverting a product of scalar pentadiagonals[1]

$$-\alpha\Delta t(\delta_{\xi\xi\xi\xi} + \delta_{\eta\eta\eta\eta})\hat{q}^n \equiv \hat{q}^* - \hat{q}^n \tag{23}$$

where

$$\left[I+\alpha\Delta tJ^{-1}(\nabla_\xi\Delta_\xi)^2J\right]\left[I+\alpha\Delta tJ^{-1}(\nabla_\eta\Delta_\eta)^2J\right]\hat{q}^* - \hat{q}^n = 0$$

It should be noted that for compatibility with the boundary conditions, a second-order smoothing is used at points adjacent to the boundary, whereas no smoothing is used at the boundary points themselves.

2.5 Numerical Stability

In explicit methods, the step size in the marching direction is bounded by the Courant-Friedrics-Lewy (CFL) condition. According to this, for block-tridiagonal matrix inversion along ξ, the AF scheme requires

$$\frac{\Delta t}{\Delta\xi}\,(\sigma_{\hat{A}})_{max} \leq 1 \tag{24a}$$

where $(\sigma_{\hat{A}})_{max}$ is the maximum spectral radius of the local eigenvalues of $\hat{A}$ and the expression given by equation (24a) is referred to as the Courant number. Similarly, for block-tridiagonal matrix inversion along η, one can write the Courant

number as

$$\frac{\Delta t}{\Delta \eta} \left(\sigma_{\hat{B}}\right)_{max} \leq 1 \tag{24b}$$

where $\left(\sigma_{\hat{B}}\right)_{max}$ is the maximum spectral radius of the local eigenvalues of B. A practical constraint in a two-dimensional problem can be written as

$$\Delta t \left[\text{max of } \frac{\sigma_{\hat{A}}}{\Delta_\xi}, \frac{\sigma_{\hat{B}}}{\Delta_\eta}\right] \leq 1 \tag{25}$$

On the basis of linear stability analysis, in implicit schemes this condition can be relaxed so that the right-hand-side constant can assume values much larger than one. In the present work, however, we have found that this was possible only for the case of supercritical operation with inviscid flow. In this case typical values were around 5 to 10. In the cases of inviscid flow with subcritical outflow boundary conditions and for viscous flow, for most of the calculation the Courant number had to be kept smaller than one to achieve numerical stability.

It should also be noted, however, that in the AF algorithm, the modulus of the amplification matrix ($|\lambda|$, ref. 1) is close to one regardless of the magnitude of Δt and therefore the scheme is only neutrally stable (for a stable scheme $|\lambda|$ should decrease with increasing Δt). Therefore, steady-state convergence cannot be accelerated by the use of very large time-steps, even where their use introduces no instability. Further information on the stability and convergence of this code can be found in reference 6.

With the inclusion of viscous terms, additional restrictions on the stability of the numerical scheme are required. Usually referred to as the "diffusive stability" restrictions, these

involve the prescription of a mesh system that ensures $Re_\Delta \tilde{-} 2$, where Re_Δ is the mesh Reynolds number. In high Reynolds number flows with $R_{e_L} >> 1$ (where L is a characteristic body dimension), this criterion will usually be met if there is fine resolution in the cross-stream, y-direction, e.g. $\Delta y \tilde{-} \delta/10$ (ref. 13). A coarse mesh in the x-direction, $\Delta x \tilde{-} L/10$ is generally accepted as adequate. In the present viscous flow calculation ($R_e = 3.28 \times 10^6$/meter) grid spacing in the η-direction varied exponentially with distance from the wall. The minimum spacing close to the cowl and ramp boundaries was around 0.3048×10^{-4} meters ($<< \delta/10$) in accord with the requirements of the turbulence model; so the requirements for diffusive stability were fulfilled.

3. OVERALL PROGRAM LOGIC

In this section the overall logic of the computer program used to solve equation (22) is summarized. The details are given in reference 1. The computational procedure starts by forming the right-hand side terms (RHS) in equation (22), first the smoothing operator then the steady part. The computational algorithm there forms Δq^* by block tridiagonal matrix inversion in ξ

$$(I + h\delta_\xi \hat{A}^n)\ \Delta\hat{q}^* = RHS \tag{26}$$

$\Delta\hat{q}^*$ is stored temporarily in $\hat{q}^{n+1}$. The procedure continues with block tridiagonal matrix inversion in η

$$(I + h\delta_\eta \hat{B}^n)\ \Delta q^n = \Delta q^* \tag{27}$$

Finally $\hat{q}^{n+1}$ is obtained from

$$\hat{q}^{n+1} = \hat{q}^n + \Delta\hat{q}^n \tag{28}$$

Note that for the two-level scheme used here, the algorithm requires two levels of data storage.

In the computer program used in this work the execution of the above outlined algorithm is performed by PROGRAM MAIN. It starts the computation by calling SUB.INITIA. This subroutine defines the physical and mathematical constants that are to be used in the computational procedure. The initial field is also specified in this subprogram. An option is provided for starting the calculation from a previously calculated (converged) field. This subroutine also calls SUB.GRID by which either a simple-stretched grid for a flat plate is computed or a previously calculated grid is read from a disc. Then SUB.XYMETS is called to evaluate the metric coefficients for the grid system.

The main program then calls SUB.EIGEN, which calculates the eigenvalues of the coefficient matrices $\hat{A}$ and $\hat{B}$; SUB.EIGEN also finds the spectral radius and finally computes the time-step from the prescribed Courant number. The optional SUB.MAP maps the P-matrix; this can either be the Jacobian of transformation or the calculated pressure field. The normalized variables and P/P_∞ of the initial field are then printed by SUB.OUTPUT. Free-stream quantities are given or computed by SUB.HARVIO.

After the initial field is prescribed and printed, the main program starts to execute the integration loop. This is done by calling SUB.STEP. This subroutine in turn calls SUB.BC to calculate data at the flow field boundaries. SUB.STEP then calls SUB.RHS which computes the steady part of the difference algorithm according to whether the flow is inviscid or viscous. If the variable INVIS is set equal to or less than zero, the program does not account for viscous effects. If INVIS > 0, SUB.VISRHS is called. The specified

variable LAMIN determines if laminar or turbulent viscous effects are to be considered. If LAMIN $\leq$ 0, SUB.MUKIN is called to calculate the molecular viscosity coefficient, μ, from Sutherland's formula. If LAMIN > 0, SUB.MUTUR is called to calculate the eddy viscosity coefficient μ_t and SUB.MUKIN is called to calculate μ. Finally, the effective viscosity $\mu_{eff} = \mu_t + \mu$ is formed. SUB.STEP then calls SUB.SMOOTH which forms the smoothing operator. The temporal differences are evaluated by SUB.DIFFER. SUB.STEP then calls SUB.FILTRX which performs the block tridiagonal matrix inversion in the ξ-direction and SUB.FILTRY which performs the block tridiagonal matrix inversion in the η-direction. Final output is furnished by subroutine SUB.HARVIO at the end of the iteration loop. The original program contains options for upwind differencing in conservative form (ref. 1) to be used in transonic flow calculations. These subroutines have not been used in the present work.

4. PROGRAM USE AND OPERATION

In this section we give a detailed description of the input information required to run a typical case. As described in Section 3, the initial field as well as values of various constants are evaluated in SUB.INITIA. This subroutine also reads the input data except for the last card, which specifies geometry (planar or axisymmetric) and type of outflow boundary. The last card is read by SUB.BC. We now list the input data cards in order:

Card No.	Format	Variables
1	815	NMAX: Maximum number of time steps JMAX: Maximum number of points along ξ KMAX: Maximum number of points along η NP: Number of time steps for calling SUB.MAP.
	815	METH: Flag for upwind differencing. If METH > 0, program skips upwind differencing. IREAD: Option for grid system. If IREAD > 0, reads grid from disc. INVIS: If INVIS > 0, program accounts for viscous effects; if INVIS = 0, the calculation is inviscid.
2	715	IREGO: If IREGO > 0, reads initial field from disc, otherwise starts from free-stream conditions. ISTORF: If ISTORF > 0, solution data stored on disc. JTAIL1: First ξ-interior point, set to 1. JTAIL2: Last ξ-interior point, set to JMAX-1. IPLOT: Index for calling plot routine.
3	315	IUPWIND: If IUPWIND > 0, skips upwind differencing. IOSCIL: For stationary airfoil set IOSCIL = 0 LAMIN: If LAMIN > 0, calculates turbulent viscosity.
4	8F10.0	CNBR: Courant number; set to about 10. DX: x-increment used in SUB.GRID. For

Card No.	Format	Variables
	8F10.0	grid read off the disc set DX = 0. DY: y-increment, as above. FSMACH: Free-stream Mach number SMU: Pseudo viscosity coefficient. Set to about 10 times the time step. EPS: Used in SUB.GRID. Here set EPS = 0. RE: Reynolds number ALPHA: Angle of attack
5	4F10.0	XOSCIL:, VARA:, VARB:, VARC: Variables required for oscillating airfoil. For the inlet flow set to zero.
6	212	LFAC: If LFAC = 1 outflow is subsonic, otherwise it is supersonic JAXI: If JAXI = 0 flow is plane 2-D, If JAXI = 1 flow is axisymmetric

(Note that axisymmetric option has been added only for the inviscid case. When calculating viscous flows, set JAXI = 0).

In starting from free-stream conditions, the number of points on the inflow boundary to be placed downstream of the ramp shock are prescribed in SUB.INITIA. Values for the variables are also prescribed in this subroutine using 2-D oblique shock theory.

The typical output of the program involves the following (described in more detail in reference 5).

(1) Tabulation of the input parameters.
(2) Printout of the Jacobian matrix as calculated from the generated grid.

(3) A map of the transformation Jacobian.

(4) Printout of the flow field variables on the cowl surface.

(5) Free-stream quantities given by SUB.HARVIO.

(6) Iteration index, physical time and time step.

(7) Maximum ERRORS occurring within the field.

(8) Values of LFAC (if LFAC > 1 outflow is subsonic) and JAXI.

(9) Mass flow ratio evaluated at various ξ-stations.

(10) Residual quantity; must converge to a small number such as $O(10^{-1})$ - $O(10^{-2})$.

(11) Line-printer plot of pressure in the computational plane.

(12) Line-printer plot of Cp on the ramp surface.

(13) Line-printer plot of Cp on the cowl surface.

(14) At time step equal to NMAX total output as furnished by HARVIO.

Note that the program that has been employed to generate the body-fitted coordinate system has been documented elsewhere (refs. 2,3).

5. PROGRAM NUMERICAL ACCURACY AND LIMITATIONS

The local accuracy of the finite difference scheme that is employed in this program is second-order both in time and space. It should be noted that the method is a conservative difference formulation, therefore its global numerical accuracy is also given by the local accuracy and is second-order in time and space. There are, however, other points that contribute to the accuracy of the numerical solution:

(a) The grid system generated has a very important effect on the overall solution. With a course grid, the shocks

(discontinuities) are not adequately resolved, and in certain cases the resulting field is totally erroneous. Near the solid walls the grid system must be properly clustered. Grids also should vary smoothly in the flow field.

(b) The overall accuracy also depends on the accuracy at the boundaries. In the present program at the flow-field boundaries it is assumed that $\hat{q}^{n+1}$ equals $\hat{q}^{n}$. Therefore on the boundaries the formal accuracy is first-order in time. Second order accuracy in space, however, is retained all through the flow field.

The major formal limitations of the program are (a) the flow field analyzed is two-dimensional, and (b) owing to the neutral stability of the method, convergence to steady state cannot be accelerated by using large time-steps. The accuracy of the results obtained in a specific application depends on the grid, as explained above, and must be evaluated ultimately by comparison with experimental data. Also the adequacy of the turbulence model used has not been addressed and requires separate study.

REFERENCES

1. Steger, J. L.: Implicit Finite Difference Simulation of Flow about Arbitrary Geometries with Application to Airfoils. AIAA Paper No. 77-665, June 1977.

2. Biringen, S. H. and McMillan, O. J.: Calculation of Two-Dimensional Inlet Flow Fields in a Supersonic Free Stream by an Implicit Marching Code with Nonorthogonal Mesh Generation - User's Manual. NASA CR-3222, January 1980.

3. Biringen, S. H. and McMillan, O. J.: Calculation of Two-Dimensional Inlet Flow Fields in a Supersonic Free Stream - Program Documentation and Test Cases. NASA CR-3221, January 1980.

4. Biringen, S., Chaussee, D. S. and McMillan, O. J.: Calculation of Inviscid Flow Fields by an Implicit Technique. AIAA Paper 80-0031, Pasadena, CA, 1980.

5. Biringen, S. and McMillan, O. J.: Calculation of Two-Dimensional Inlet Flow Fields by an Implicit Method Including Viscous Effects - Program Documentation and Test Cases. NASA CR-3414, 1981.

6. Biringen, S. and McMillan, O. J.: An Implicit Method for the Calculation of Inlet Flow Fields. NASA CR-3413, 1981.

7. Viviand, H.: Conservative Forms of Gas Dynamic Equations, La Recherche Aerospatiale, No. 1, 1974, pp. 65-68

8. Baldwin, B. S., and Lomax, H.: Thin-Layer Approximation and Algebraic Model for Separated Flows. AIAA Paper 78-257, Huntsville, Alabama, 1978.

9. Cebeci, T.: Calculation of Compressible Turbulent Boundary Layers with Heat and Mass Transfer. AIAA Paper 70-741, Los Angles, California, 1970.

10. Beam, R. and Warming, R. F.: Implicit Factored Schemes for Conservation Laws. AIAM-AMS Proc., Vol. 11, 1977.

11. Beam, R. and Warming, R. F.: An Implicit Factored Scheme for the Compressible Navier-Stokes Equations. AIAA Paper No. 77-645, June 1977.

12. Steger, J. L. and Bailey, H. E.: Calculation of Aileron Buzz. AIAA Paper No. 79-0134, January 1979.

13. MacCormack, R. W., and Lomax, H.: Numerical Solution of Compressible Viscous Flows, Amer. Rev. Fluid Mechs., Vol. 11, p. 289, 1979.

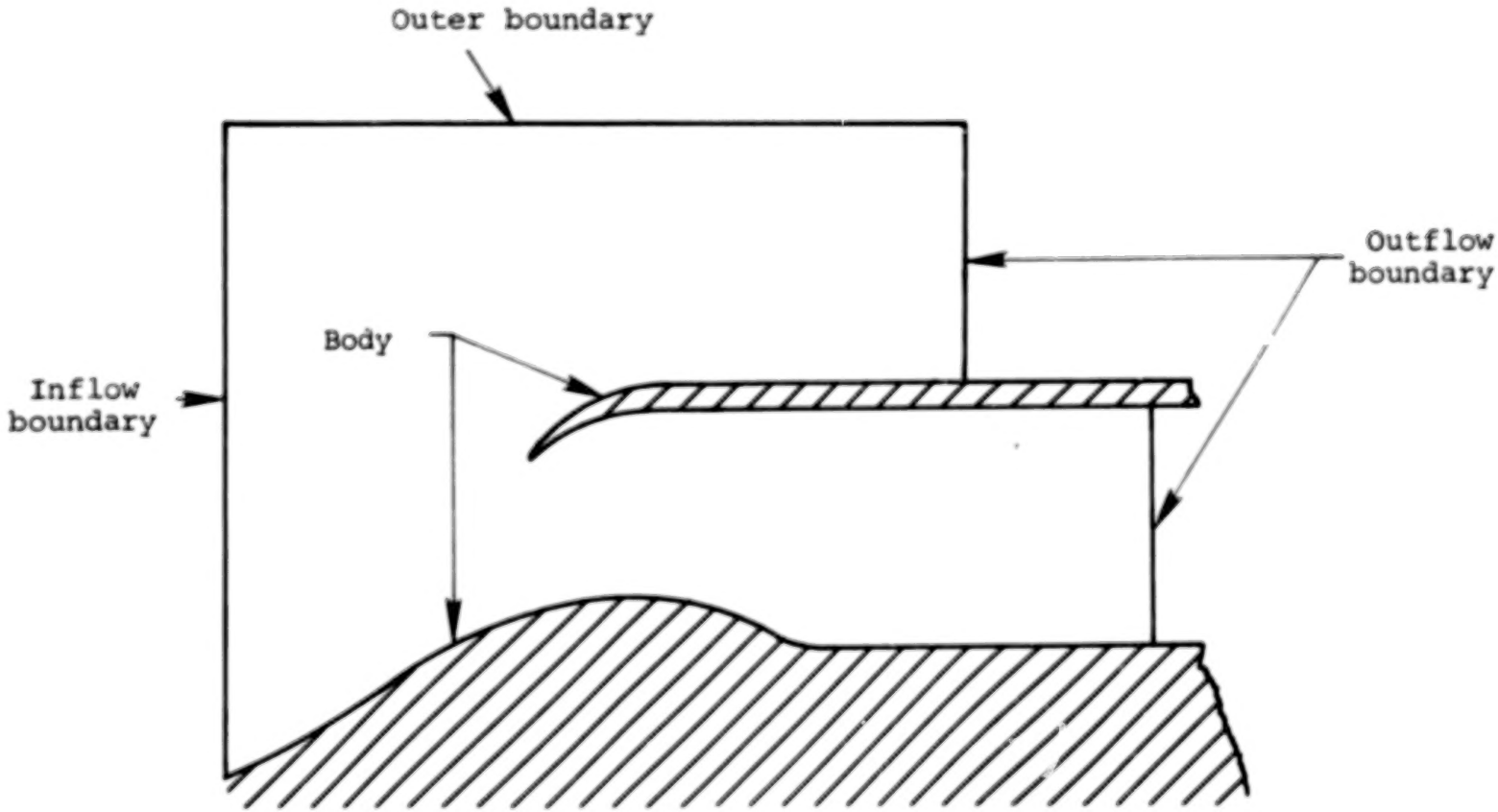

Figure 1.- Flow-field boundaries.

1 Report No	2 Government Accession No	3 Recipient's Catalog No
NASA CR-3412		

4 Title and Subtitle	5 Report Date
CALCULATION OF TWO-DIMENSIONAL INLET FLOW FIELDS BY AN IMPLICIT METHOD INCLUDING VISCOUS EFFECTS - USER'S MANUAL	May 1981
	6 Performing Organization Code: 611/C
7 Author(s): Sedat Biringen and Oden J. McMillan	8 Performing Organization Report No.: NEAR TR 231
	10 Work Unit No
9 Performing Organization Name and Address: Nielsen Engineering & Research, Inc. 510 Clyde Avenue Mountain View, California 94043	11 Contract or Grant No.: NAS1-15951
	13 Type of Report and Period Covered: Contractor Report 9/12/79 - 11/30/80
12 Sponsoring Agency Name and Address: National Aeronautics and Space Administration Washington, DC 20546	14 Sponsoring Agency Code

15 Supplementary Notes

Langley Technical Monitor: Wallace C. Sawyer
Topical Report

16 Abstract

Inlet flow fields for airbreathing missiles are calculated by the adaptation of a two-dimensional computational method developed for the flow around airfoils. A supersonic free stream is assumed to allow the forebody calculation to be uncoupled from the inlet calculation. The inlet calculation employs an implicit, time-marching finite-difference procedure to solve the thin-layer Navier-Stokes equations formulated in body-fitted coordinates. The mathematical formulation of the problem and the solution algorithm are given. Numerical stability and accuracy as well as the initial and boundary conditions used are discussed. Instructions for program use and operation along with the overall program logic are also given.

17 Key Words (Suggested by Author(s))	18 Distribution Statement
Calculation method Inlets Supersonic flow Viscous flow	Unclassified - Unlimited Subject Category 02

19 Security Classif (of this report)	20 Security Classif (of this page)	21 No. of Pages	22 Price
Unclassified	Unclassified	23	A02

For sale by the National Technical Information Service, Springfield, Virginia 22161

NASA-Langley, 1981

END

July 29, 1981